

Quarter Wave Plate for Q-band optics in Yebes 40m radio-telescope

F. Tercero, Ó. García-Pérez

CDT Technical Report 2020-08

Observatorio de Yebes
19080, Guadalajara (Spain)
E-mail: f.tercero@oan.es

Abstract– The Q-band receiver front-end currently installed in the 40m radio-telescope delivers dual linear polarization, which is not properly indicated for standard VLBI observations. A Quarter Wave Plate (QWP) placed in the optical path, in front of the receiver, provides a suitable solution to switch from linear to circular polarizations without the need of any other component inside the cryostat at cold temperature. Straight grooved surfaces on low permittivity plastics (e.g. Teflon or Polyethylene) present biaxial dielectric constant to implement in affordable thickness such QWP. In addition, the use of triangular-shaped grooves can improve the reflection coefficient, but at the cost of adding machining complexity. This report presents the design, construction and measurements of a QWP based on triangular-shaped grooves. The characterization of the fabricated QWP in an open-waveguide optical bench has allowed testing the actual return and dielectric losses, and the cross-polarization levels of the beam transformed from linear to circular polarization. Instructions to install it properly in the radio-telescope are also included.



March, 2020

Contents

Contents	3
1 Introduction	4
2 Specifications	5
3 Electrical design	7
3.1 Material characterization.....	7
3.2 Tool preparation	8
3.3 Groove profile	8
3.4 Full wave simulation	9
3.5 Dielectric losses.....	11
3.6 Mechanical design and interface	11
4 Experimental measurements	12
5 Conclusion	15
References	16
Appendix A. Mechanical interface from Q-band optics	17
Appendix B. Final groove design.	18
Appendix C. Mechanical design	18
Appendix D. Instrucciones de montaje	20

1 Introduction

The *Quarter Wave Plate (QWP)* is a type of polarization transducer that produces 90° differential phase shift between polarizations. QWPs are characterized by a fast and a slow axis. The phase velocity is different for the two orthogonal polarizations. The QWP thickness determines the phase shift at a single frequency.

There are anisotropic materials that naturally have this birefringence property, like for example the crystal quartz ($n=2.1$, $\Delta n=0.05$, $\tan\delta\approx 0.1\cdot 10^{-4}$). However, this high permittivity and losses result in a poorly matched and lossy plate, as well as in a quite thick plate because of its modest birefringence.

On the other hand, isotropic materials can be geometrically modified to change the propagation properties of the incident polarized electric field. For instance, thermoplastics like *Teflon (PTFE)* or *Polyethylene (PE)* have better permittivity and losses and they are easily machinable. As a result, artificially anisotropic layers can be designed by means of grooved strips on the plastic surface. These profiled grooves are commonly rectangular in sectional view.

In grooved QWPs, perfect 90° phase shift happens at a single frequency and it is degraded quickly along the bandwidth. On the other hand, perfect matching is not possible for both polarizations simultaneously at a given frequency. This is the most limiting factor for plate performance where, once the material (and subsequently the losses) has been chosen, deviations from 90° narrows the bandwidth of the plate.

This report presents the design and characterization of a QWP for the Q-band receiver of the Yebes 40-m radio-telescope. In order to improve the impedance matching of the QWP, a design based on triangular-shaped grooves has been proposed, although it is mechanically more difficult to build compared to a regular rectangular-shaped [1]. In a previous research, both Teflon and PE with rectangular and triangular grooves prototypes were built and fully characterized. The results presented in this document corresponds with the one that presented the best performance, which was the one based on a triangular grooved PE design (internal code: YQWP-Q-02-002).

2 Specifications

The design should be based on the “best effort” basis. The current frequency bandwidth for VLBI observations is limited to 500 MHz. However new aim on VLBI observations (both European and American) is to reach 32 Gbit/sec sampling rate, based on the capabilities of the samplers of the backends (i.e. DBBC3 or several R2DBE). This results in 4 GHz instantaneous bandwidth for 2 bit and 2 polarization receivers. Nevertheless, for the design of the QWP at Q-band it is not a big deal because it corresponds to 10% relative bandwidth at a 40 GHz typical frequency, which can be covered by the previously proposed dielectric grooved structure. Table 1 summarizes the frequency bandwidth in this design.

		Current Observations with EVN and KVN	New plans for Global VLBI
Q band VLBI bandwidth	[GHz]	42.75 - 43.25	41.00 - 45.00

Table 1. Bandwidth specifications.

The QWP will be placed in the optical path of Q-band receiver. Room enough has been envisaged for a plate thickness less than 42 mm (view 0 for details about the mechanical interface). Beam diameter between M3 and M4 mirrors, where the QWP will be placed, must be higher than 140 mm to prevent beam truncation, as it is shown in Fig. 1 [2].

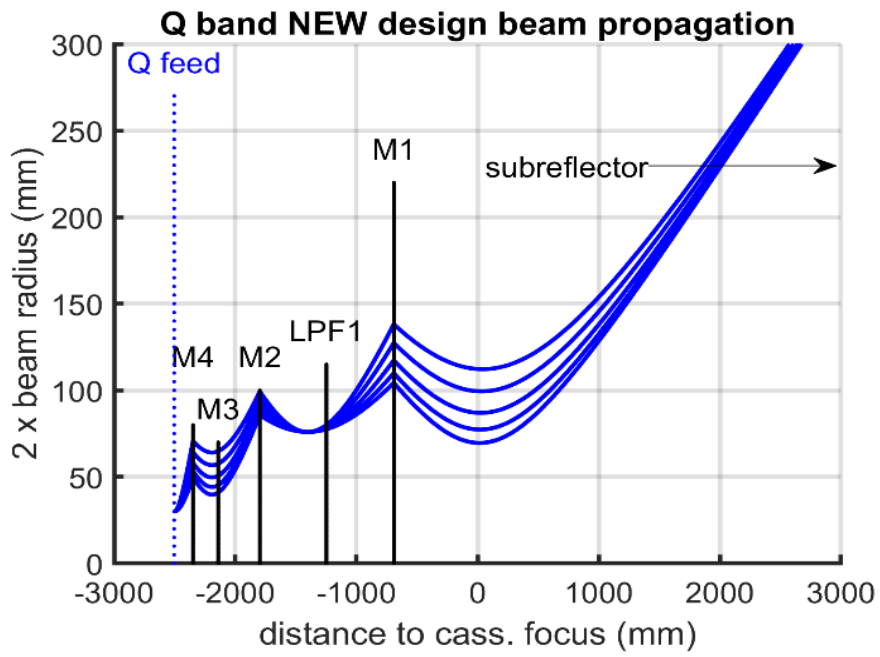


Fig. 1. Beam propagation for Q-band receiver at -35 dB level from maximum. Several lines depict the frequencies 31, 35, 40, 45 and 50 GHz.

3 Electrical design

The electrical design of the QWP has been performed based on full-wave simulations and optimizations on CST software. Nevertheless, prior to the electrical simulation is necessary to characterize both the material and the tool for machining, since they are constraints for the fabrication and the electrical performance.

3.1 Material characterization

Polyethylene (PE) material is chosen because of its low dielectric constant and losses, as well as its easiness to manufacture and low cost. Depending on the manufacturing process, different densities may be purchased with identical dielectric constant ($\epsilon_r=2.3$). In this case, *Ultra High Molecular Weight Polyethylene (UHMWPE)* is chosen because of its null water absorption coefficient and better machinability [3].

The slab of material to be machined was previously characterized to measure its dielectric constant. The measurement was done following the procedure described in [4], after adapting the test bench Q-band measurements using suitable standard gain horns (*SGH*) for such bandwidth (model *QGH-QPRR00*, from Quinstar). Those feeds provide lower gain than feeds originally used for W-band. It results in a slightly smaller beam (-8.7 dB gaussian beam) in the *Sample Under Test (SUT)* of 28.5 mm. Dielectric lenses were identical to the W-band case but the distance from the feeds to the lenses had to be reset to the new feed beam-waist.

The complex permittivity number is extracted from the 2-port open waveguide measurements applying the three available methods. The results are obtained from the average of the three methods (i.e. *NIST*, *TEF* and *SNI*) to calculate the complex dielectric constant and standard deviation associated (Table 2).

UHMWPE (slab 27.950 mm)	Average (NIST-TEF-SNI)	STD
ϵ_r	2.295	0.004
$\tan\delta/10^{-4}$	1.1	19

Table 2. Measurement of the UHMWPE sample.

Loss tangent determination disagrees between the three methods described above. Average may be taken as an approximate figure to estimate losses and equivalent noise temperature.

3.2 Tool preparation

The tool used to machine the grooves on the dielectric sample is a custom design from a modified hard-metal old-drill grip. It is a sharp mid-cone to engrave the triangular shape on the dielectric material (Fig. 2). Although in a first step its profile was geometrically measured, the real curve on the dielectric was slightly different. Therefore, the actual carved profile was measured on the dielectric and was later used as a constraint for the electrical design.

3.3 Groove profile

The parameters defining the geometry of the QWP are shown in Fig. 3. The dimensions of the tool fix both θ and s parameters in the electrical design. Consequently, the free parameters for the optimization are both the depth of the corrugation (d) and the inner dielectric core thickness (e). Final figures for the groove are in 0.

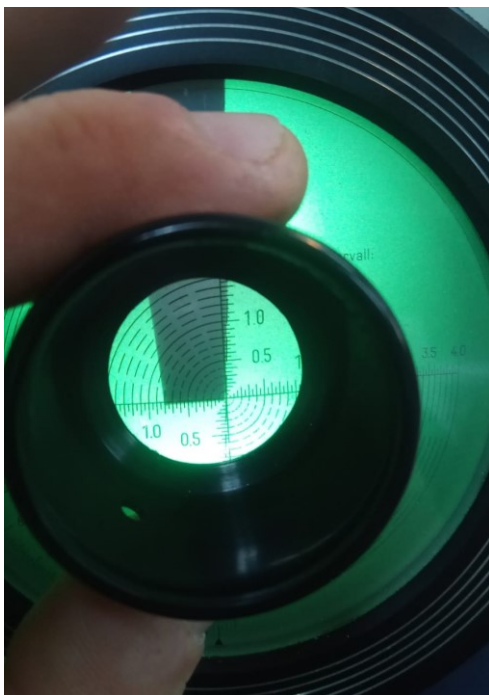


Fig. 2. Optical inspection of the tool profile.

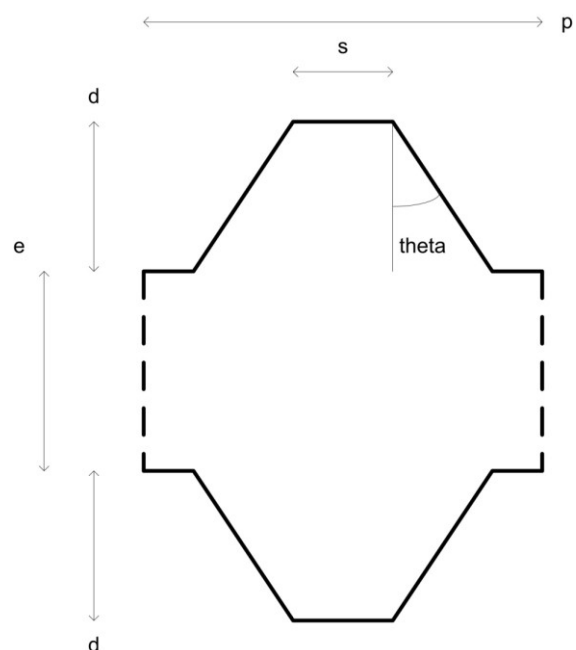


Fig. 3. Sectional view profile of a single corrugation.

3.4 Full wave simulation

UHMPE is simulated as a free loss dielectric material in CST. The simulation comprises the unit cell only. Electric field vector is 45° with respect to the direction of the dielectric strips. In this configuration, linear polarization is converted into circular in an ideal QWP. For this reason, the port configuration is linear/circular for the input/output ports.

The return loss of the QWP remains in same polarization, and values better than -24dB are expected from simulation, as it is shown in Fig. 4. Out of the working bandwidth, it is worth to realize that reflection losses are better than -15dB. It is convenient to have this figure outside of the used band for the QWP, because LNA bandwidth is wider and it might decrease its noise performance or even show resonances if the input port is not well matched.

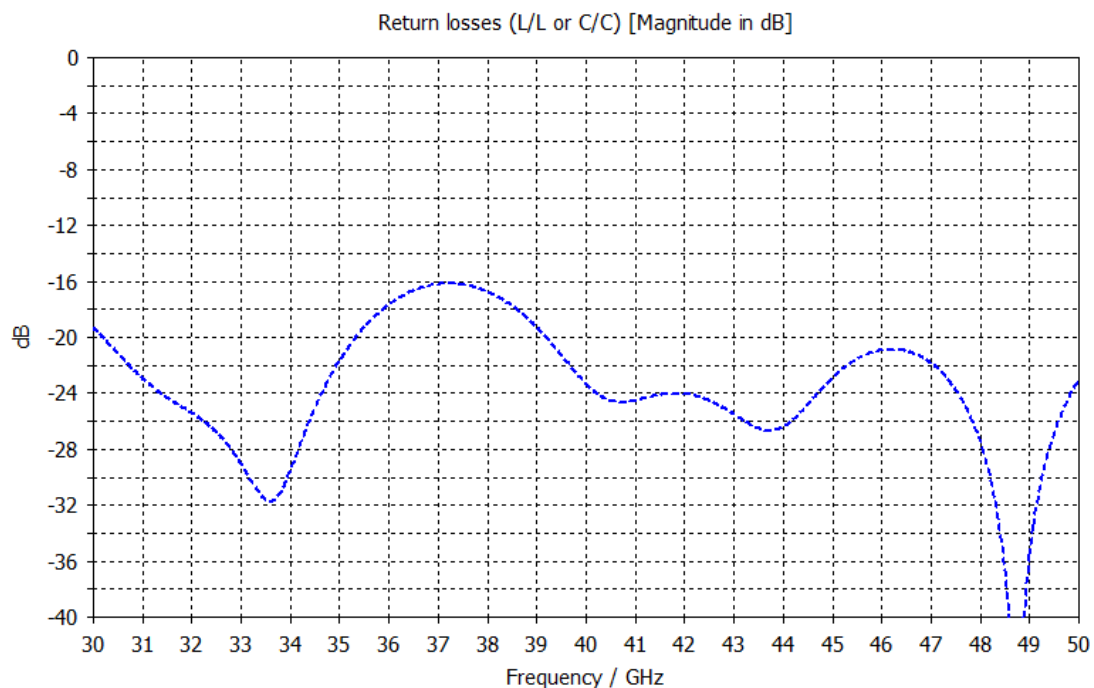


Fig. 4. Simulated return losses of the QWP. There is not a change in the state of polarization, if linear polarization is incident on the plate the reflected wave remains linear polarized.

The transmitted wave through an ideal QWP would change the polarization state from linear to circular, or vice versa. Any non-ideal behavior in the change of the polarization state is seen as a loss in the transmission. The simulated transmission from linear to circular polarization is shown in Fig. 5. The complementary transmission from linear to linear is shown in Fig. 6.

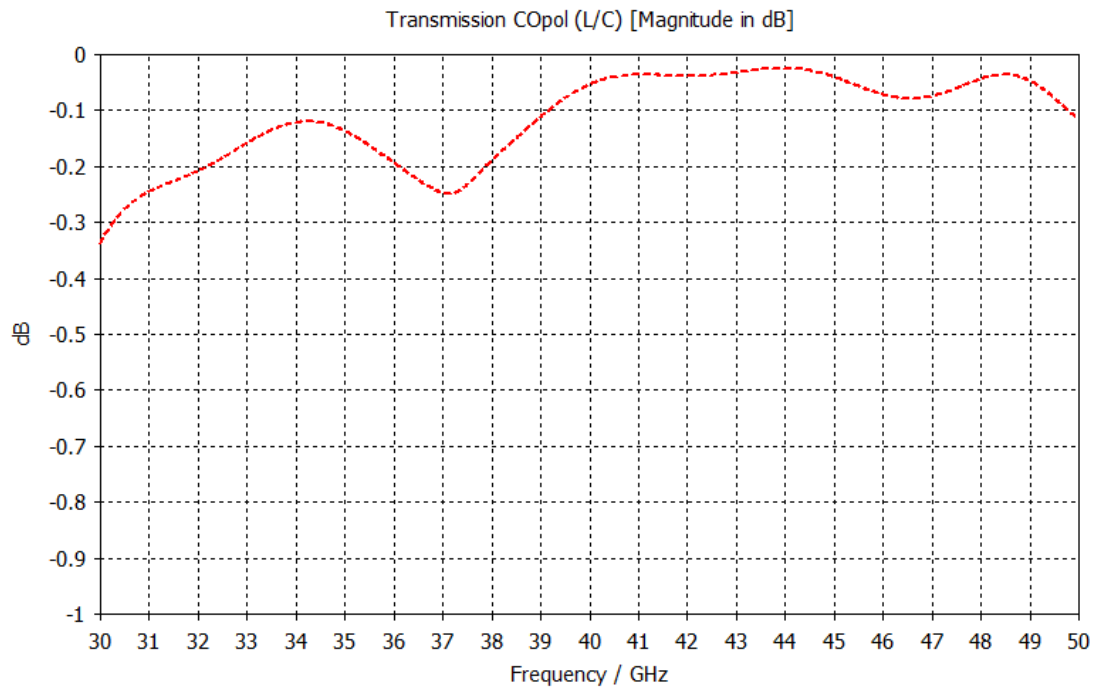


Fig. 5. Simulated transmission loss for linear to circular conversion.

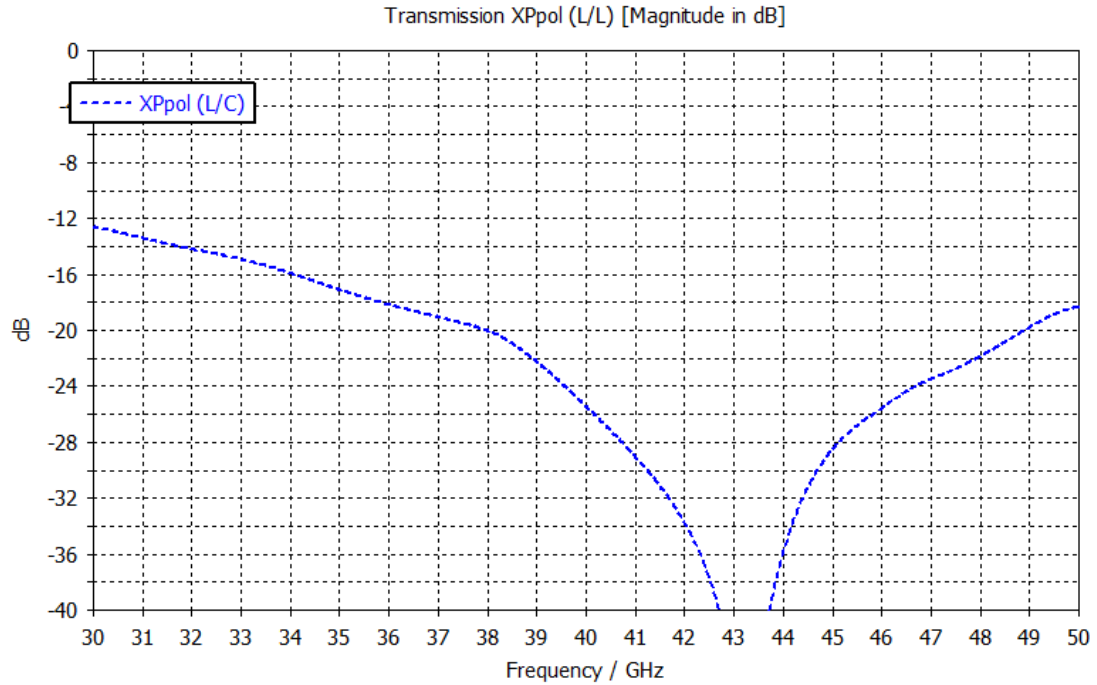


Fig. 6. Simulated transmission loss for linear to linear (or circular to circular). Rejection of the undesired polarization.

3.5 Dielectric losses

The dielectric losses come up from the dielectric slab of the material. To calculate them, the dielectric tangent loss from section 3.1 is used with the thickness of the designed plate.

Dielectric losses at 43 GHz	L_{dB}	[dB]	0.0044
Equivalent noise temperature at 43 GHz	T	[K]	0.3

Table 3. Equivalent temperature noise estimation from thickness and dielectric losses.

As it can be observed in Table 3, the dielectric loss contribution to the noise temperature is negligible in comparison with total receiver equivalent noise temperature.

3.6 Mechanical design and interface

The plate is milled on a UHWPE slab with circular external rim. It is attached to a squared aluminum frame with several through holes to prevent the slab from getting deformed after machining.

Aluminum frame has 4 tapped holes on each side. Two of them are at 100 mm distance to interface with the optical support of Q-band optics. Two holes at 30 mm are prepared to the measurement bench. There are drills in the four sides because during the measuring process, the plate must be rotated 90° as it is explained in section 4.

Mechanical drawings are presented in 0.

4 Experimental measurements

For the experimental measurements of the QWP prototype, the optical bench at Q-band is set up as in section 3.1. The ports of the optical bench are both in linear polarization because port network signal is launched with SGHs. In this configuration, the QWP is set up with grooves tilted 45° from linear polarization. The measurement of the reflection can be measured directly, because both launched and reflected waves are linearly polarized. However, it is not possible to have a direct measurement for the transmission and polarization transformation from linear to circular as it was obtained from simulations in section 3.4.

To obtain transmission results equivalent to the ones shown in section 3.4, both transmission and polarization transformation can be calculated indirectly, from direct measurements with two linear ports. In this case, the plate's grooves must be set up parallel and perpendicular to the linear polarization in two consecutive measurements. These two results must be averaged: directly to have reflection measurement; with relative shift of $+90^\circ$ to have co-polar desired component; and with relative shift of -90° to have cross-polar undesired component.

The measured reflection parameter, obtained from the direct and indirect experimental setups, are shown in Fig. 7. Both measurements are compared with the simulated results. Actual measurements are shifted in frequency less than 0.75 GHz with respect to the expected performance. Furthermore, measured reflection figures are slightly better than expected in simulation. It might be because the experimental setup is sensitive to misalignments of the sample for the reflection measurement, which might underestimate this value. Direct and indirect measurements disagree 4 dB in the worst-case frequency. At the EVN observation frequencies the reflection is better than -22dB.

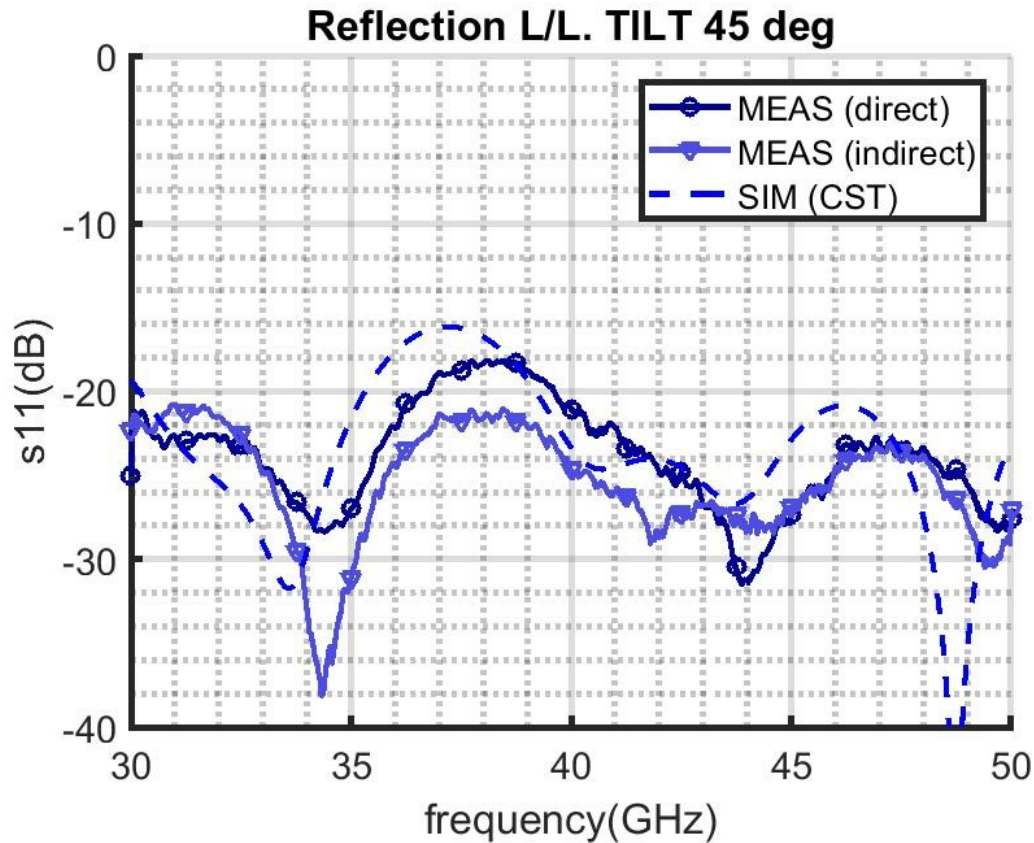


Fig. 7. Reflection loss for linear to linear (or circular to circular). Comparison between direct and indirect measurements and simulation results.

Fig. 8 shows the calculated transmission from indirect measurements in both linear polarizations. Co-polar and cross-polar transmissions are both compared with the simulations. There is a slight frequency offset between measurements and simulated results, which agrees with the offset also observed in the measured reflection parameter. Simulation agrees well with measurements, except for values under -24dB where the cross-polar transmission is not resolved properly at such low levels. It seems to be an artifact in measurement set-up because:

- Total power balance between s-parameters agrees with minimum levels in cross-polar transmission at this 43-44 GHz frequency.
- Losses are not worse in that frequency.

A plausible explanation for that lack of resolution in the cross-polar level is related with the set-up configuration, since calibration might be inaccurate due to internal reflections from the lenses. The lenses were originally designed to work at W-band with proper grooving in the Teflon surfaces at these frequencies. Although calibration should ideally correct instrumental reflections at any frequency, including Q-band measurements, it might be inaccurate below some low level that sets the floor for the measurement. Even though, cross-polar measurement levels are acceptable for this design.

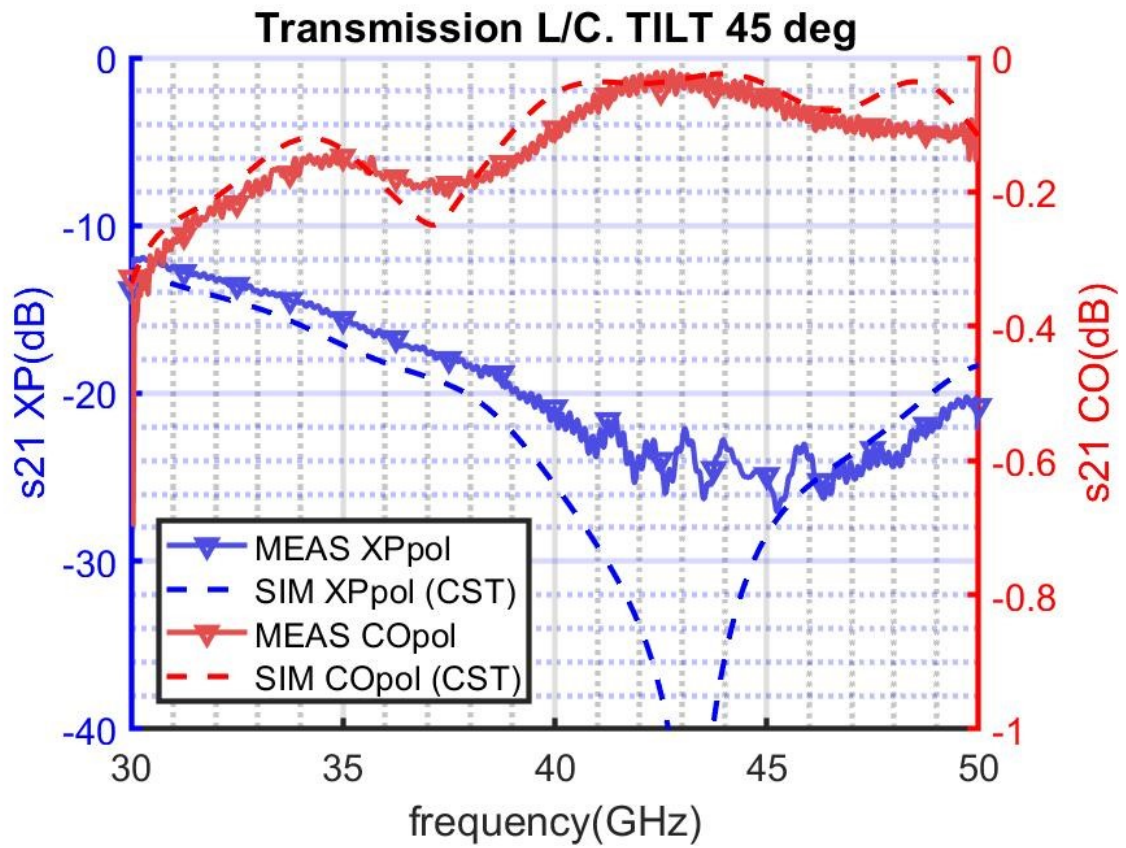


Fig. 8. Transmission loss for linear to circular. Indirect measurements averaged to show actual behavior of the plate.

5 Conclusion

A new QWP to transform from linear to circular polarization in the Q-band receiver of the radio-telescope has been manufactured and measured. Best performance obtained for a center frequency around 43 GHz guarantees commitment to the EVN and KVN specifications.

In order to tune the design, previous measurements of the dielectric constant have allowed having a plate with a less than 2% frequency shift. It is an acceptable mismatch considering the large bandwidth. The determination of the losses has not been as accurate as the determination of the dielectric constant. Nevertheless, it is negligible in the overall performance of the receiver, estimated in 0.004dB.

Final design was carried out taking as constraints both measured dielectric constant and tool preparation for machining. These two actions have minimized the errors in the final prototype.

Measurements with an optical bench have allowed to check that the actual performance agrees with simulated results. Loss in polarization transformation has been measured to be -0.05dB.

The plate might be used out of the specified bandwidth because worst figure in reflection is -18dB in the entire Q-band receiver bandwidth. Attending to polarization purity requirements, the plate might be used along the entire Q-band.

Among the possible future lines, one consists on investigating the reasons why cross-polar measurement in the open waveguide test bench is losing accurateness for levels below -24dB.

References

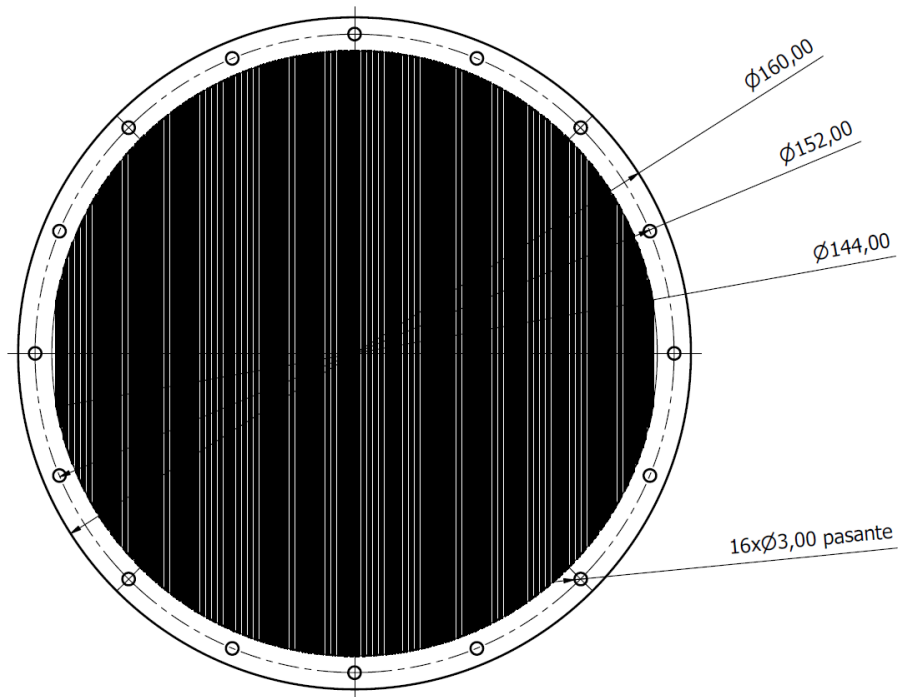
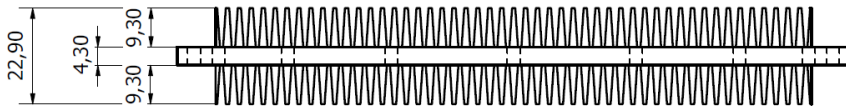
- [1] P. F. Goldsmith, Quasioptical Systems. Gaussian Beam Quasioptical Propagation and Applications, New York: IEEE Press Series on RF and Microwave Technology, 1998.
- [2] F. Tercero y O. Garcia-Perez, «Broadband K-Q-W feed system for the 40 meters Yebes radio telescope,» de *Proceedings of the 2019 21st International Conference on Electromagnetics in Advanced Applications, ICEAA 2019, Granada, 2019*.
- [3] Wikipedia, "Ultra-high-molecular-weight polyethylene," [Online]. Available: https://en.wikipedia.org/wiki/Ultra-high-molecular-weight_polyethylene. [Accessed 12 03 2020].
- [4] O. Garcia-Perez, F. Tercero and S. Lopez-Ruiz, "Free-space W-band setup for the electrical characterization of materials and mm-wave components," CDT Technical Report 2017-9, 2017.

Appendix B. Final groove design.

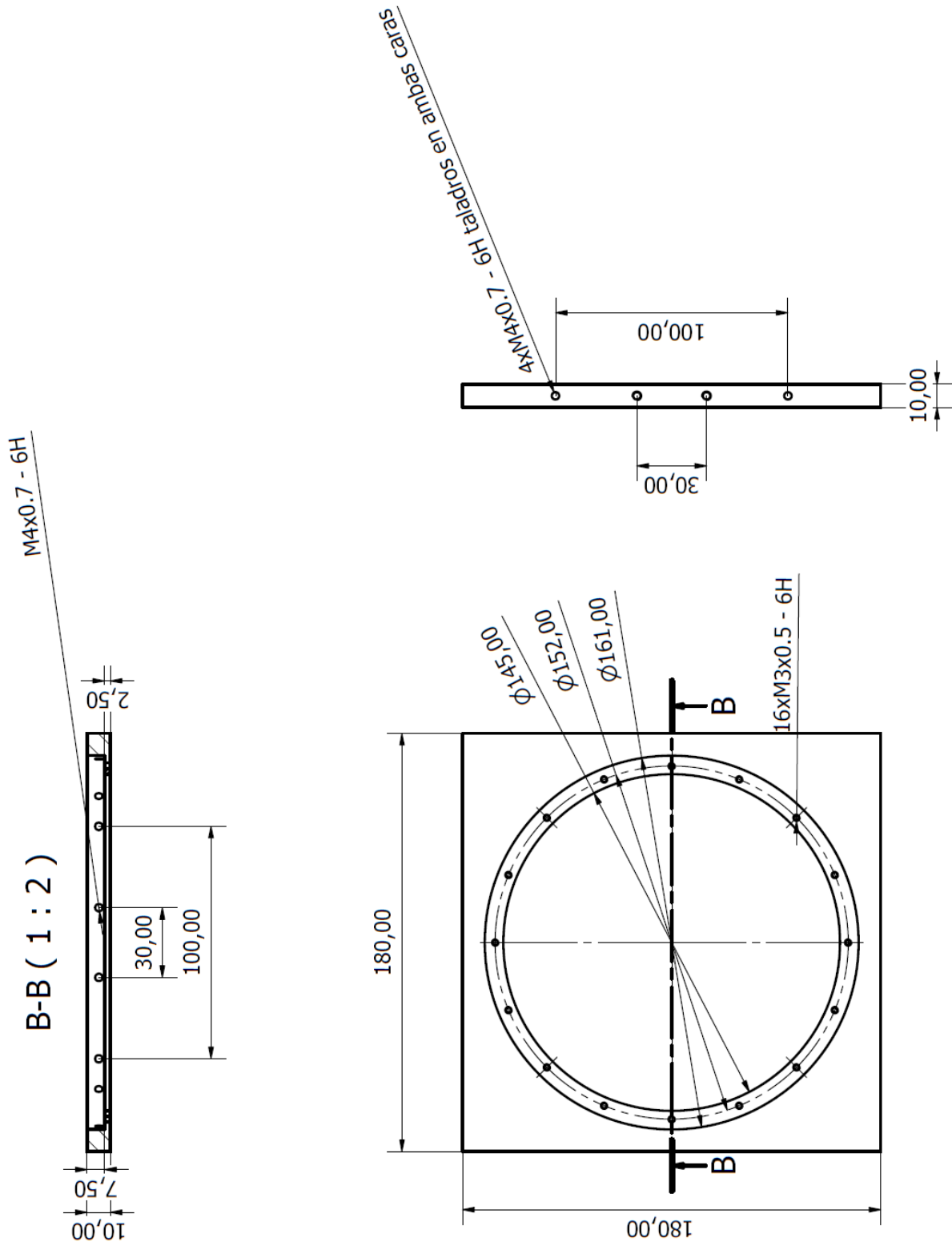
This appendix has been intentionally removed. For further information contact with authors on f.tercero@oan.es.

Appendix C. Mechanical design.

- Polyethylene plate



- Squared aluminum frame.



Appendix D. Instrucciones de montaje

- El polarizador de banda Q usado en el radiotelescopio de 40 metros es el numerado como **YQWP-02-002**. De forma alternativa se pueden usar los modelos YQWP-02-001 y YQWP-03-001, que tienen características similares al recomendado, aunque se desaconseja su uso ya que los datos de este informe se refieren al primero de ellos.
- Se harán coincidir las marcas del polarizador con las marcas de la estructura de la óptica de los espejos. Durante la (des)instalación se tendrá cuidado de no rozar el propio polarizador como los espejos superior e inferior ya que entra muy ajustado. **En ningún caso hacerlo entrar de forma forzada**, informar en caso de que se encuentren dificultades en la instalación.
- Una vez desinstalado guardar en su caja protectora de metacrilato junto con el resto de elemento ópticos de la cabina de receptores.
- Las polarizaciones **vertical/horizontal** del receptor se corresponden con las polarizaciones **izquierda/derecha** respectivamente, del radiotelescopio.